

# Emergent energy scales in magnonic systems with relative motion

Daigo Oue<sup>1,2</sup>

<sup>1</sup>RIKEN Centre for Advanced Photonics, RIKEN, Saitama 351-0198, Japan

<sup>2</sup>The Blackett Laboratory, Imperial College London, London SW7 2AZ, United Kingdom

E-mail: [daigo.oue@gmail.com](mailto:daigo.oue@gmail.com)

## Abstract

Relative motion between interacting systems can generate emergent energy scales that are absent in isolated systems. While uniform motion can be eliminated by a Galilean transformation, relative motion between interacting systems generally cannot. In the presence of characteristic spatial structures, relative motion gives rise to a Doppler frequency scale determined by the characteristic wavevector of the excitation and the relative velocity of the system. This emergent scale provides a fundamental mechanism for driving nonequilibrium phenomena in moving systems. In particular, the emergent energy scale is determined by how the relative motion probes the spatial structure of the relevant excitation.

In this tutorial, we illustrate these ideas using magnonic systems as a concrete platform. We first discuss motion-induced magnon transport between relatively moving ferromagnets, in which the Doppler frequency serves as an effective nonequilibrium bias in the perturbative regime. This mechanism produces magnon currents even in the absence of conventional driving forces such as temperature gradients or chemical potential differences.

We then introduce motion-induced parametric instabilities. When the emergent scale becomes sufficiently large to resonantly create magnon pairs, the perturbative description breaks down, and the magnonic vacuum becomes unstable. Above a critical velocity threshold, spontaneous magnon-pair creation emerges, resulting in strongly enhanced transport and nonequilibrium dynamics.

Connections to related phenomena, including quantum friction, Cherenkov emission, and Zeldovich superradiance, are also highlighted. The concept of an emergent energy scale provides a unifying framework for understanding transport phenomena and instabilities in quantum systems with relative motion.

## Glossary

*Magnon, Doppler effect, Transport phenomena, Instability, Galilean transformation, PT symmetry*

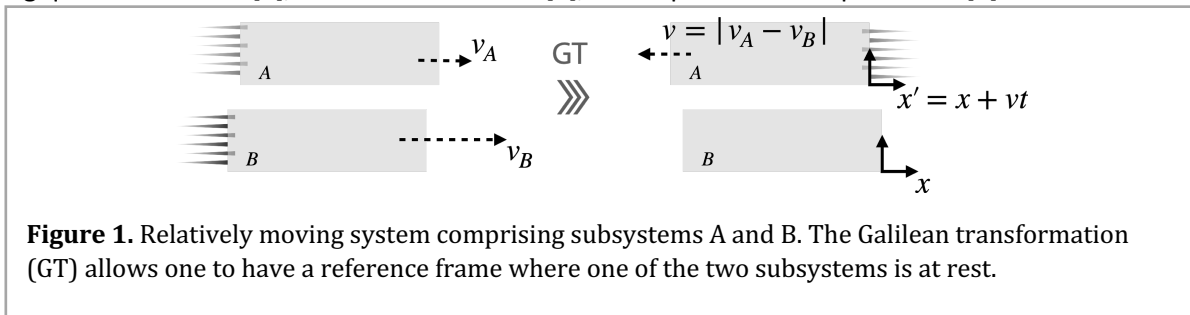
## Introduction

Relative motion is ubiquitous in nonequilibrium physics, appearing in a wide range of systems from sheared interfaces to counter-flowing plasmas. Such relative motion gives rise to a wide variety of nonequilibrium phenomena and has attracted considerable interest across many branches of physics. At first sight, this nonequilibrium nature may seem counterintuitive, since uniform motion of an isolated system has no observable consequence: it can always be eliminated by changing the reference frame and is therefore indistinguishable from equilibrium.

The situation changes qualitatively when multiple interacting systems move relative to one another. Although each subsystem may undergo uniform motion, no single inertial frame can simultaneously bring all interacting subsystems to rest. In this sense, relative motion is piecewise uniform but not globally uniform. It may therefore be regarded as a discontinuous velocity field, providing a fundamentally nonequilibrium platform for interacting systems.

Indeed, relative motion induces a broad range of nonequilibrium phenomena, most notably transport processes and dynamical instabilities. For example, sheared interfaces experience friction through momentum transport across the interface [1], whereas counter-flowing plasmas exhibit dynamical instabilities associated with the softening of collective modes [2]. Despite their different manifestations, both ultimately originate from the same piecewise but globally non-uniform nature of relative motion. One of the central messages of this tutorial is that both can be understood in terms of an emergent energy scale arising from relative motion.

In this tutorial, we take magnonic systems as a simple and instructive platform to illustrate these ideas. In particular, we show how relative motion, via an emergent energy scale, gives rise to motion-induced transport phenomena [3][4] and dynamical instabilities [5] in interacting ferromagnets. The underlying physical picture is applicable well beyond magnonics, and we briefly discuss connections to related phenomena in other fields, including quantum friction [1], Cherenkov emission [6], and superradiant amplification [7].



### Emergent energy scales induced by relative motion

Relative motion alone does not define an emergent frequency scale. Indeed, the relative speed  $v = |\mathbf{v}|$  has the dimension of velocity and therefore cannot be directly compared with the characteristic frequencies of a physical system. To generate a frequency scale, the velocity must be combined with a characteristic length scale  $\ell$  of the system. Dimensional analysis then immediately suggests the emergent frequency scale  $\Delta = 2\pi v/\ell$ , which represents the simplest frequency scale associated with relative motion.

The characteristic length is naturally identified with a component of the wavevector of an elementary excitation: Consider two interacting systems in relative motion and choose the inertial frame in which one of them is at rest, as illustrated in Fig. 1. In this frame, the other subsystem moves with the relative velocity  $\mathbf{v}$ . An elementary excitation on the moving subsystem with a dispersion relation  $\omega_{\mathbf{k}}$  has the phase factor  $\exp[i(\mathbf{k} \cdot \mathbf{x}' - \omega_{\mathbf{k}}t)]$ , where the coordinates satisfy  $\mathbf{x}' = \mathbf{x} + \mathbf{v}t$ . Expressing the phase in terms of the stationary coordinate gives  $\mathbf{k} \cdot \mathbf{x}' - \omega_{\mathbf{k}}t = \mathbf{k} \cdot \mathbf{x} - (\omega_{\mathbf{k}} - \mathbf{k} \cdot \mathbf{v})t$ , showing that the excitation is observed with the Doppler-shifted frequency  $\omega_{\mathbf{k}} \rightarrow \omega_{\mathbf{k}} - \mathbf{k} \cdot \mathbf{v}$ .

The emergent frequency scale predicted by the dimensional argument is therefore identified as  $\Delta = k_v v$  with the projected wavenumber  $k_v = \mathbf{k} \cdot \mathbf{v}/|\mathbf{v}|$ . This is nothing but the Doppler shift of a finite-wavevector excitation. This immediately explains why the uniform mode ( $\mathbf{k} = 0$ ) is unaffected by relative motion, whereas finite- $\mathbf{k}$  excitations experience a frequency shift determined by the projection of the relative velocity onto the wavevector. The above discussion is based on a Galilean transformation and therefore applies in the non-relativistic regime. For relativistic velocities, the frequency shift should instead be obtained from the Lorentz transformation.

Once interactions between the two subsystems are introduced, the emergent frequency scale should appear in the interaction. In general, we can consider two types of resonance conditions: difference-frequency and sum-frequency conditions,

$$\omega_b - \omega_a = \Delta, \quad \omega_b + \omega_a = \Delta. \quad (1)$$

Which resonance condition becomes relevant depends on the interaction channel. Two fundamental excitations (bosonic mode on each subsystem) are described by the creation and annihilation operators  $a_k^\dagger, a_k$  and  $b_k^\dagger, b_k$ . The interaction Hamiltonian can therefore be classified according to whether it exchanges excitations between the two subsystems or simultaneously creates (or annihilates) excitation pairs. The most general bilinear interaction between two bosonic modes can therefore be constructed from four operator products,

$$a_k b_{-k}, \quad a_k b_k^\dagger, \quad a_k^\dagger b_k, \quad a_k^\dagger b_{-k}^\dagger. \quad (2)$$

Since the interaction Hamiltonian must be Hermitian, these four terms naturally combine into two independent interaction channels,

$$H_{\text{ex}} = \sum_k g_{\text{ex}} (a_k^\dagger b_k + a_k b_k^\dagger), \quad H_{\text{nc}} = \sum_k g_{\text{nc}} (a_k^\dagger b_{-k}^\dagger + a_k b_{-k}), \quad (3)$$

where  $g_{\text{ex}}$  and  $g_{\text{nc}}$  are interaction strengths associated with the two interaction channels. The first channel conserves the total number of excitations by exchanging an excitation between the two subsystems, whereas the second channel simultaneously creates or annihilates a pair of excitations (see Fig. 2).

Suppose that the excitation represented by  $a$  ( $b$ ) belongs to the moving (stationary) subsystem. Then, the corresponding free evolutions of the annihilation operators are  $a_k \sim \exp[-i(\omega_a - k_x v)t]$  and  $b_k \sim \exp(-i\omega_b t)$ . Here, the dependence on the wavevector  $\mathbf{k}$  in the dispersion relation is left implicit. We further assume that the relative velocity is given by  $\mathbf{v} = v\mathbf{u}_x$  with  $\mathbf{u}_x$  the unit vector in the  $x$  direction. With these conditions, the unperturbed Hamiltonian is given as

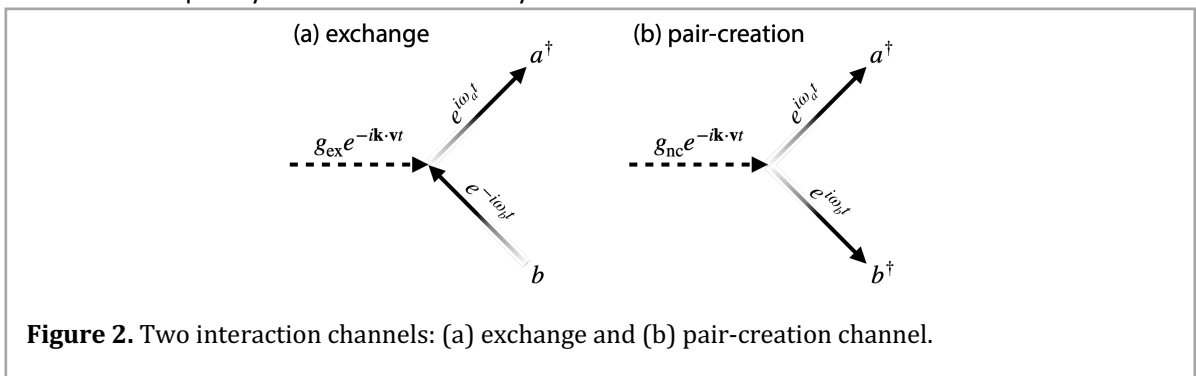
$$H_0 = \sum_k \{(\omega_a - k_x v) a_k^\dagger a_k + \omega_b b_k^\dagger b_k\}. \quad (4)$$

Going to the interaction picture [e.g.  $O \rightarrow O(t) = e^{+iH_0 t} O e^{-iH_0 t}$ ], we can write

$$H_{\text{ex}}(t) = \sum_k g_{\text{ex}} e^{i(\omega_a - \omega_b - k_x v)t} a_k^\dagger b_k + \text{h. c.}, \quad H_{\text{nc}}(t) = \sum_k g_{\text{nc}} e^{i(\omega_a + \omega_b - k_x v)t} a_k^\dagger b_{-k}^\dagger + \text{h. c.} \quad (5)$$

The origin of the two resonance conditions (1) now becomes apparent: The phase factor associated with each channel contains exactly the resonance conditions anticipated above. Resonance occurs when the corresponding phase factor becomes stationary; therefore, the exchange-conserving (non-conserving) channel is resonantly enhanced under the difference-frequency (sum-frequency) condition.

The following two sections discuss how the difference-frequency resonance gives rise to transport phenomena, whereas the sum-frequency resonance leads to dynamical instabilities.



### Transport driven by emergent energy

When the emergent frequency scale is sufficiently small, the excitation-conserving interaction channel becomes the relevant one (so we consider  $H = H_0 + H_{\text{ex}}$  in this section). This interaction is resonantly enhanced under the difference-frequency condition and serves as an effective nonequilibrium bias that drives transport. It transfers an excitation from one subsystem to the other while conserving the total number of excitations, and its physical consequence is therefore naturally a transport phenomenon. In conventional transport, nonequilibrium is typically created by temperature or chemical-potential differences. Here, relative motion provides an alternative source of nonequilibrium through the emergent frequency scale generated by the Doppler shift. Consequently, the transport can be understood perturbatively as a response to this effective nonequilibrium bias.

As an example, let us consider two identical ferromagnetic insulators, one moving at a constant velocity while the other remains at rest. The magnon dispersion relation is given by

$$\omega_{a,b} = Dk^2 + \omega_0, \quad (6)$$

where  $D$  is the spin-wave stiffness and  $\omega_0$  denotes the Zeeman energy. Note that we consider only the  $x$  direction for simplicity, as it is the direction that is most significantly affected by the Doppler effect  $k_x v$ . Applying time-dependent perturbation theory with respect to the exchange interaction  $H_{\text{ex}}$ , the spin transfer carried by magnons between the two magnets can be evaluated analytically [3][4], yielding

$$I_s = 4(\hbar g_{\text{ex}})^2 \int \Im \left( \frac{2S_0/\hbar}{\omega - (\omega_a - kv) + i\Gamma} \right) \Im \left( \frac{2S_0/\hbar}{\omega - \omega_b + i\Gamma} \right) [n_B(\omega_b) - n_B(\omega_a - kv)] dk d\omega, \quad (7)$$

where  $\Gamma$  is a phenomenological damping constant for the magnon,  $S_0$  is the magnitude of the localised spin, and  $n_B$  is the Bose distribution function. In the resulting expression (7), the product of fractions represents the spectral overlap between two magnons, and we have the population difference. It is clear that relative motion effectively shifts both the magnon spectrum and the magnon population of the moving subsystem. The transport is therefore governed by the combined effect of the spectral overlap and the population imbalance between the two magnets, leading to a net magnon (spin) current across the interface. The detailed derivation can be found in Refs. [3][4].

An interesting consequence is that the spin transfer is proportional to the second order of the relative velocity. This can be understood from the fact that the Doppler shift always appears through the combination  $kv$ . The first-order contribution vanishes after the integration over the wavevector because it is odd in  $k$ , leaving the leading contribution proportional to  $v^2$ . This is consistent with the intuitive picture that the transport is driven by the kinetic energy associated with the relative motion, which is itself proportional to  $v^2$ .

### Instabilities driven by emergent energy

When the emergent frequency scale is sufficiently large, the excitation-nonconserving interaction channel becomes the relevant one (so we consider  $H = H_0 + H_{\text{nc}}$  in this section). This interaction is resonantly enhanced under the sum-frequency resonance condition and simultaneously creates or annihilates pairs of excitations. Unlike the exchange channel discussed in the previous section, the consequence here is not transport between two subsystems but the amplification of collective excitations. In this regime, the emergent frequency scale no longer acts merely as an effective nonequilibrium bias. Instead, it provides the energy required for pair creation through an effective parametric drive. Once the pair-creation process becomes resonant, the excitation population grows exponentially, eventually leading to a dynamical instability.

Before explicitly treating the interaction, it is useful to estimate the threshold using the resonance condition. For two identical ferromagnets with the magnon dispersion relation,  $\omega_{a,b} = Dk^2 + \omega_0$ , the sum-frequency resonance condition,  $\omega_a + \omega_b - vk = 0$ , gives

$$2Dk^2 - vk + 2\omega_0 = 0. \quad (8)$$

This quadratic equation has real solutions only when

$$v^2 - 16D\omega_0 > 0, \quad (9)$$

which gives the threshold estimate  $v_c \approx 4\sqrt{D\omega_0}$ .

This result is consistent with dimensional analysis: since the stiffness  $D$  has the dimension of  $\text{m}^2/\text{s}$  and the Zeeman energy  $\omega_0$  has the dimension of  $1/\text{s}$ , the combination  $\sqrt{D\omega_0}$  naturally defines the characteristic velocity scale of the magnonic system. This argument only uses the resonance condition and does not yet include the interaction strength. It identifies the velocity regime in which magnon-pair creation becomes energetically allowed.

To determine the actual stability of the interacting system, we consider the equations of motion for the magnon creation and annihilation operators. Collecting the operators into the vector, the Heisenberg equations can be written as [5]

$$i \frac{\partial}{\partial t} \begin{pmatrix} a_k \\ b_{-k} \\ a_k^\dagger \\ b_{-k}^\dagger \end{pmatrix} = \begin{pmatrix} \omega_a - kv & 0 & 0 & g_{\text{nc}} \\ 0 & \omega_b & g_{\text{nc}} & 0 \\ 0 & -g_{\text{nc}} & -\omega_a + kv & 0 \\ -g_{\text{nc}} & 0 & 0 & -\omega_b \end{pmatrix} \begin{pmatrix} a_k \\ b_{-k} \\ a_k^\dagger \\ b_{-k}^\dagger \end{pmatrix} \quad (10)$$

The stability is determined by the eigenvalues of the Liouvillian [the 4-by-4 matrix in Eq. (10)], which are

$$\pm \frac{1}{2} \left( kv \pm \sqrt{(\omega_a + \omega_b - kv)^2 - 4g_{\text{nc}}^2} \right). \quad (11)$$

When the square root becomes imaginary, one of the eigenvalues acquires a positive imaginary part, and the corresponding mode grows exponentially in time. The growth rate is therefore determined by

$$\Gamma_k = \frac{1}{2} \sqrt{4g_{\text{nc}}^2 - (\omega_a + \omega_b - kv)^2} \quad (12)$$

in the parameter region where the quantity inside the square root is positive. For the parabolic magnon dispersion, this condition can be written as  $(2Dk^2 - vk + 2\omega_0)^2 < 4g_{\text{nc}}^2$ . Equivalently, the instability occurs when  $v > v_c = 4\sqrt{D(\omega_0 - g_{\text{nc}})}$ , which reduces to the resonance-based threshold ( $v_c \approx 4\sqrt{D\omega_0}$ ) in the weak-interaction regime ( $g_{\text{nc}} \ll \omega_0$ ). The detailed derivation and stability analysis can be found in Ref. [5].

Although the Liouvillian above already allows us to determine the instability, a sequence of unitary transformations brings it into a simpler  $PT$ -symmetric form [5],

$$\begin{pmatrix} \omega_a - kv & 0 & 0 & g_{\text{nc}} \\ 0 & \omega_b & g_{\text{nc}} & 0 \\ 0 & -g_{\text{nc}} & -\omega_a + kv & 0 \\ -g_{\text{nc}} & 0 & 0 & -\omega_b \end{pmatrix} \mapsto \begin{pmatrix} +ig_{\text{nc}} & -kv/2 & 0 & 0 \\ -kv/2 & -ig_{\text{nc}} & 0 & 0 \\ 0 & 0 & -ig_{\text{nc}} & +kv/2 \\ 0 & 0 & +kv/2 & +ig_{\text{nc}} \end{pmatrix} \quad (13)$$

This form makes the connection to non-Hermitian physics transparent (the block matrices have the same form as the typical matrix discussed in the context of  $PT$  symmetry in the non-Hermitian physics [8]): the nonconserving interaction gives rise to balanced gain and loss, while the Doppler effect couples the two modes. The onset of the instability can therefore be interpreted as spontaneous  $PT$ -symmetry breaking. Below the threshold, the eigenvalues remain real; above the threshold, they form complex-conjugate pairs, and the positive imaginary part gives the exponential amplification discussed above.

### Connections to other motion-induced phenomena

The viewpoint developed in this Tutorial is not specific to magnonic systems but applies more broadly to interacting bosonic systems that support collective excitations, including phonons, plasmons, photons, and exciton-polaritons. In particular, the pair-creation channel discussed in Section 4 is closely related to the microscopic mechanism of quantum friction, in which relative motion induces correlated photon pairs across moving interfaces, thereby giving rise to momentum transfer and frictional forces [9]–[14]. Closely related pair-generation mechanisms also underlie Zel'dovich superradiance [7] and quantum Cherenkov emission [15]–[17], where kinetic energy associated with relative motion is converted into propagating excitations. A closely related picture also emerges in the dynamical Casimir effect, where an effective parametric drive generates correlated

photon pairs from vacuum fluctuations [18]–[21]. We hope that the viewpoint developed here—namely, understanding relative motion through the emergent frequency scale and the associated resonance conditions—will prove useful for understanding and designing a broad range of motion-induced nonequilibrium quantum phenomena.

## Summary

In this tutorial, we have discussed motion-induced phenomena in magnonic systems and shown how relative motion can drive nonequilibrium dynamics. We have seen that relative motion between interacting magnetic systems generates an emergent frequency scale associated with the Doppler effect. This scale is determined by how the relative motion probes the spatial structure of magnonic excitations, providing a common framework for understanding transport phenomena and dynamical instabilities.

We have first considered motion-induced magnon transport between relatively moving ferromagnets. In this regime, the Doppler shift acts as an effective nonequilibrium bias, producing an imbalance in magnon populations and driving magnon tunnelling between the two systems. Remarkably, this transport can occur even in the absence of conventional driving mechanisms such as temperature gradients or chemical potential differences.

We have then discussed a qualitatively different regime that emerges when the Doppler frequency becomes sufficiently large. Under these conditions, magnon pairs can be resonantly excited, causing the perturbative transport picture to break down. The magnonic vacuum becomes unstable, leading to spontaneous magnon-pair creation and enhanced transport phenomena above a critical velocity threshold.

Finally, we have highlighted connections to a broader class of motion-induced phenomena, such as quantum friction. These examples illustrate that emergent energy scales generated by relative motion provide a unifying perspective on transport phenomena and instabilities in moving systems.

## Acknowledgements

D.O. is supported by the RIKEN special postdoctoral researcher program. This work was supported by JSPS KAKENHI Grant Numbers JP26K17783 and 26H00686 and by RIKEN Incentive Research Project.

## References

- [1] Dedkov GV and Kyasov AA 2017 *Physics-Uspekhi* **60** 559
- [2] Sydoruk O, Shamonina E, Kalinin V and Solymar L 2010 *Phys. Plasmas* **17** 102103
- [3] Oue D and Matsuo M 2022 *Phys. Rev. B* **105** L020302
- [4] Oue D and Matsuo M 2024 *physica status solidi (b)* **261** 2300469
- [5] Uto T and Oue D 2025 *Phys. Rev. B* **112** 024305
- [6] Ginzburg VL 1996 *Physics-Uspekhi* **39** 973
- [7] Zel'Dovich YB 1971 *Sov. JETP Lett.* **14** 180
- [8] El-Ganainy R, Makris KG, Khajavikhan M, Musslimani ZH, Rotter S and Christodoulides DN 2018 *Nat. Phys.* **14** 11
- [9] Pendry JB 1997 *J. Phys.: Condens. Matter* **9** 10301
- [10] Volokitin A and Persson BN 2007 *Rev. Mod. Phys.* **79** 1291
- [11] Silveirinha MG 2014 *New J. Phys.* **16** 063011
- [12] Brevik I, Shapiro B and Silveirinha MG 2022 *Int. J. Mod. Phys. A* **37** 2241012
- [13] Oue D, Pendry JB, and Silveirinha MG 2024 *Phys. Rev. Research* **6** 043074
- [14] Oue D, Shapiro B and Silveirinha MG 2025 *Phys. Rev. B* **111** 075403
- [15] Maghrebi MF, Golestanian R, and Kardar M 2013 *Phys. Rev. A* **88** 042509
- [16] Roques-Carmes C, Rivera N, Joannopoulos JD, Soljačić M, and Kamnitzer I 2018 *Phys. Rev. X* **8** 041013,
- [17] Fares H and Almokhtar M 2019 *Phys. Lett. A* **383** 1005
- [18] Moore GT 1970 *J. Math. Phys.* **11** 2679
- [19] Dodonov VV 2010 *Phys. Scr.* **82** 038105
- [20] Wilson CM, Johansson G, Pourkabirian A, Simoen M, Johansson JR, Duty T, Nori F and Delsing P 2011 *Nature* **479** 376
- [21] Lähteenmäki P, Paraoanu GS, Hassel J and Hakonen PJ 2013 *Proc. Natl. Acad. Sci. USA.* **110** 4234